Brodogradnja/Shipbuilding Volume 65 Number 2, 2014

Dario BAN
Branko BLAGOJEVIĆ
Bruno ČALIĆ

ISSN 0007-215X
eISSN 1845-5859

ANALYTICAL SOLUTION OF GLOBAL 2D DESCRIPTION OF SHIP GEOMETRY WITH DISCONTINUITIES USING COMPOSITION OF POLYNOMIAL RADIAL BASIS FUNCTIONS

UDC 629.5(012)
Original scientific paper

Summary

One of the well-known problems in the curves and surfaces reconstruction theory regarding global analytic object description, besides the description of its curvature changes, inflexions and non-bijective parts, is the existence of oscillations near point discontinuities in the middle of the range and at the boundaries of the description. In the ship geometric modelling, ship hull form is usually described globally using parametric methods based on B-spline and NURB-spline, for they have general property of describing discontinuities. Nevertheless, they are not enabling direct, exact calculation of ship's geometric properties, i.e. the calculation of the integrals for determining geometric and other geometry properties or the intersection with water surface. Because of above mentioned, the predominant way of computing geometric properties of the ships is still numerical computation using Simpson integration methods, which also dictates mesh based description of an observed geometry.

Analytical solution of global 2D description for ship geometry with discontinuities will be shown in this paper, using the composition of polynomial RBFs, thus solving computational geometry problems, too.

Key words: *ship geometry; meshless; piecewise; discontinuities; Gibbs phenomenon; Runge phenomenon; polynomial RBFs;*

1. Analytical description of discontinuities

From the beginning of naval architecture as science, in the works of its founders Chapman, [1], Euler, [2], Taylor, [3], and others, there have been the efforts of analytical description of ship geometry using polynomials, that has not been completely efficient in solving all analytical geometry problems. One of the main problems in an analytical global description of arbitrary ship geometry is the description of its discontinuities, where large curve oscillations occurs near discontinuities (Gibbs phenomenon), and on the boundaries of the description (Runge phenomenon), as shown on Figure 1. Besides knuckles of the curve, the boundaries of the description are the discontinuities, too, with one singular branch.

Because of that, described object is usually divided in segments, and the calculation of its geometric properties is separated in parts, or the calculations are performed using numerical methods like in numerical integration. In doing so, no other information but points are used.

On the other side, when analytical description of the geometry is done, it cannot describe discontinuities without their explicit, direct designation using supervised learning, and appropriate curve break elimination. Therefore, besides the data pairs in the input data set X and output data set Y, the analytical description requires additional geometry information like the derivations in defined input points, the position of discontinuities, and so on. Figure 1 shows the example of the wedge with branches defined by unit circle, described by Lagrange's polynomials for equidistant points.

One of the biggest advantages of parametric methods based on B-splines and NURB-splines, [4], and the reason why they are widely used in geometric modelling compared to direct description methods, is their ability to describe discontinuities of the curves and surfaces. Nevertheless, the same property of RBF description will be shown in this paper, i.e. the possibility of discontinuities description using RBF networks, with much higher accuracy. The RBF description has the basic property of piecewise description, as shown in 2D ship geometry description using RBF with polynomial precision, [5], and therefore it is assumed that it is possible to change their bases, in order to change the description curvature near knuckles, as will be shown later in the text.

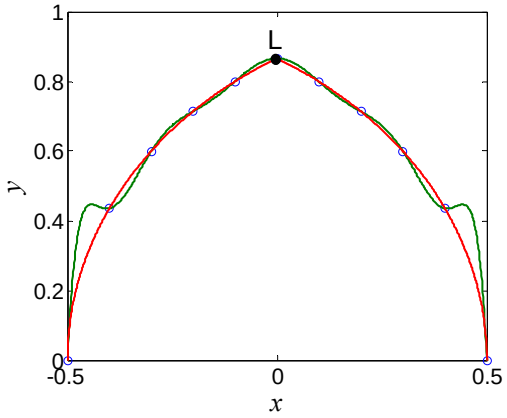

Figure 1 The wedge with branches, defined by unit circle, and described by Lagrangian polynomials for equidistant points, with $N = 11$ (L is the break point)

Two methods for the solution of the description of the curves with discontinuities are shown in the dissertation, [6]: Elastic Shift Method and Composition of Radial Basis Functions with Dense Points near Discontinuities, with later been more efficient and therefore chosen to be represented and explained in this paper. In order to examine the efficiency of the global 2D RBF description method to be shown in this paper, two arbitrary test frames with several discontinuities are chosen: 1. The test frame of the car-truck carrier with flat side and camber, and 2. The test frame of the planning boat with several knuckles and curved camber, as described in the Appendix. Those test problems represent complex description problems of actual ship geometries to be solved.

The required global and local accuracies for those ship frames descriptions are set to the values of 10^{-4}, in order to fulfil further integration requirements for solving ship's computational geometry problems as the main goal of the geometry description.

2. The curve and surface reconstruction

The problem of the curve or some surface reconstruction is the problem of the determination of the function f based on the input data set $X \equiv \{x_j, j = 1,\ldots, N\}$ and output data set points $Y \equiv \{y_j, j = 1,\ldots, N\}$, on the range $[a, b]$, where $a = x_1$ and $b = x_N$, that describes the curve or surface defined by observed points. There are a larger number of methods defined for that purpose which are approximating, or interpolating, in their nature. Regarding the ways of learning, the reconstruction process can be divided in the non-supervised and supervised learning procedures. The former procedure takes input and output data sets only as sufficient for the description of the object to be reconstructed, while the latter needs additional information about inflexion points, extremes, the discontinuity points L, curvatures ρ and belonging derivations.

2.1 The conditions for the existence of analytical functions

The basic condition for the existence of analytical functions is the existence of the bijection, i.e. the surjection and the injection, between input data set X and output data set points Y. The function also must agree with Taylor series developed around every input data set point, [7]. Analytic functions are for example: polynomials, exponential functions, trigonometric functions u rectangle Cartesian (Decartes) coordinate system, and radial basis functions that will be observed in this paper.

Bijection

For some function it can be said it is analytical if it satisfies the conditions of surjection and injection between input data set points X and output data set Y, i.e. there exists one-to-one correspondence that gives one unique functional value for each input point value.

The analytical function can be generally defined as $f : \Omega \to IR^l \subseteq C^\infty$, i.e. continuous function mapping from the subset of d-dimensional real space $\Omega \subseteq IR^d$ to some l-dimensional real space IR^l where bijective mapping exists.

2.2 Radial basis function networks

In general, radial basis function networks are defined as the linear combination of basis functions, which depend on the distance between input data set points, **x**, and the points of centres, **t**, around which the function is developed. They can be further described as weighted sum of radial basis functions translated around the points called centres, whose number depends on mathematical procedure chosen for object representation. Therefore, RBF network can be represented in the form:

$$\mathbf{y} = f(\mathbf{x}) = \sum_{i=1}^{O} w_i \Phi_i\left(\left\|x, t_i\right\|\right), \mathbf{x} \in \Omega \subseteq IR^d, \mathbf{y} \in IR^l \tag{1}$$

where **x** is input variables data points set, **y** is output variables data points set, **t** is the set of O centres radial basis functions are developed for, **w** is the matrix of the weight coefficients, d is the dimension of input data set, and l is the dimension of output data set.

By analogy with neural networks, RBFs are defined explicitly as the functional relationship between input and output data sets, as shown on Figure 2, with the network matrix **H** as the interpolating/approximating matrix with the elements $H_{ji} = \Phi_i\left(\left\|x_j, t_i\right\|\right)$.

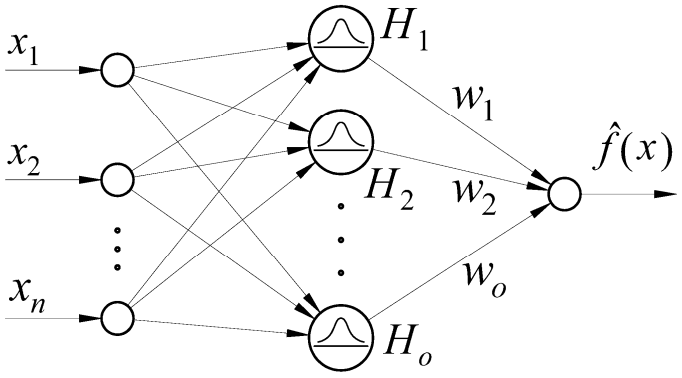

Figure 2 Single-layered, Feed-forward RBF Neural Network

Theoretical foundations for the RBF definition as the linear combination of basis functions come from the Reproducing Kernel Hilbert Spaces (RKHS) theory, introduced by Nachman and Aronszajn, [8]. In RKHS there are positive definite kernels defined that ensure the point convergence and ortho-normal basis defined by:

$$\hat{f}(x) = \sum_{i=1}^{O} w_i K(x, x_i) = \sum_{i=1}^{O} w_i B_i = \sum_{i=1}^{O} w_i \Phi_i(x) \tag{2}$$

where $x_j, j = 1,...,N; x \in IR^s$ is input data set, K are reproduction kernels, B_i are basis functions, Φ_i are radial basis functions, t_i are RBF development centres with $i = 1,...,O$, where O is the number of centres, w_i are weight coefficients of RBF network, φ are radial basis functions based on the norm between input data points and the points of centres, and $\hat{f}(x)$ is generalized interpolating/approximating function.

The main advantage of RBFs is that they are the solution of scattered data interpolation problem, the solution obtained by determination of weight coefficient vector/matrix **w**, using inversion of interpolating matrix **H** as:

$$\mathbf{w} = \mathbf{H}^{-1} \cdot \mathbf{y} \tag{3}$$

Furthermore, in the example of the RBFs applicability in geometry description, [5], there are conditionally positive definite functions used for global 2D RBF interpolating description of ship's geometry, using RBFs with polynomial precision, in the form:

$$\hat{f}(x) = \sum_{i=1}^{N} w_i \varphi(\|x, t_i\|) + \sum_{k=1}^{M} \omega_k p_k(x), \quad x \in IR^s \tag{4}$$

where φ are radial basis functions, and $p_1 \dots p_M$ are basis in $M = \binom{s+m-1}{m-1}$ dimensional linear polynomial space Π_{m-1}^s.

Thus, in the most general form of the solution of the system of linear equations is:

$$\begin{bmatrix} \mathbf{H} & \mathbf{P} \\ \mathbf{P}^T & 0 \end{bmatrix} \begin{bmatrix} \mathbf{w} \\ \boldsymbol{\omega} \end{bmatrix} = \begin{bmatrix} \mathbf{y} \\ \mathbf{0} \end{bmatrix} \tag{5}$$

where $H_{ji} = B_j(x_i)$, $j, i = 1, \dots, N$, $P_{jl} = p_l(x_i)$, $l = 1, \dots, M$, $\mathbf{w} = [w_1, \dots, w_N]^T$, $\boldsymbol{\omega} = [\omega_1, \dots, \omega_M]^T$, $\mathbf{y} = [y_1, \dots, y_N]^T$, and **0** is null-vector of length M.

Regarding RBF networks with L_2 norm, they have optimal recovery property, i.e. they belong to native reproductive Hilbert spaces (RKHS), [8], and are the best approximators, [9], that minimize the oscillations of the boundaries.

2.3 Polynomial Radial Basis Functions with L_1 norm

Nevertheless above stated characteristics of standard RBFs, the possibility of the application of Polynomial RBFs (PRBFs) with L_1 norm will be investigated here also, for they have computationally efficient and robust form, together with high precision, as shown in dissertation, [6]. They are generally defined as:

$$f(x)=\sum_{j=1}^{N} w_i\left(\left|x-t_i\right|^{\beta}+c\right),\ \beta\in IR\setminus 2\cdot IN \tag{6}$$

with shape parameter c set outside of polynomial brackets, and function exponent β defined in the whole space real numbers IR restricted for even integers, as shown on Figure 3, below.

Figure 3 shows β – RMSE sensitivity diagram of the RBF description of Franke's 1D function, [10], where all but even integer values of Polynomial Radial Basis Function exponents β from real space IR give acceptable RMSE values. It is obvious that odd integer values for PRBF exponent β are acceptable, thus enabling integer polynomial functions.

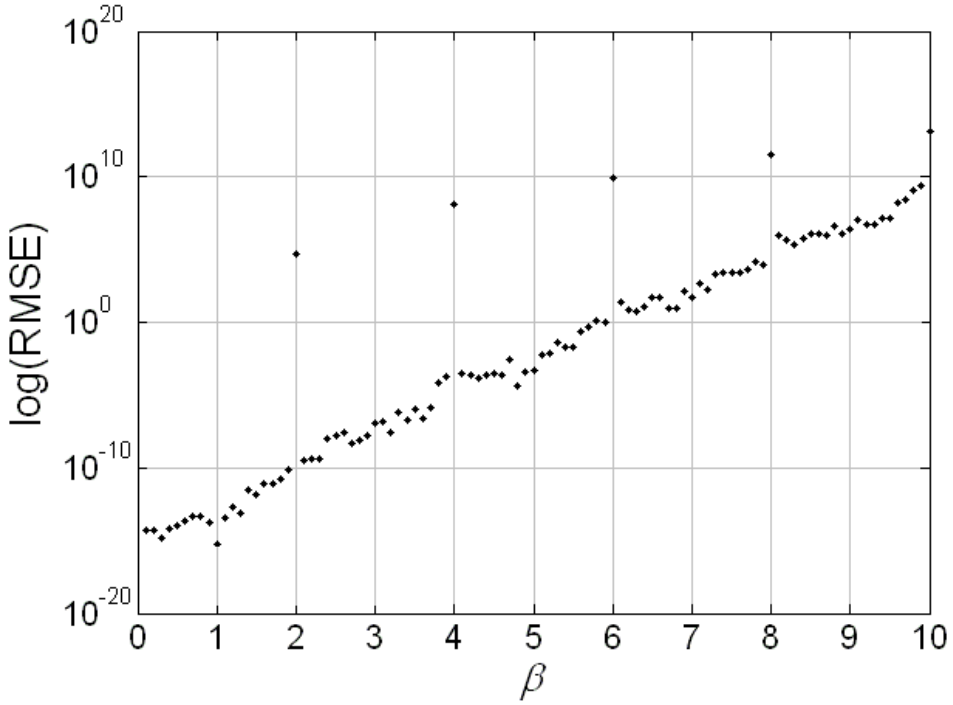

Figure 3 The sensitivity diagram β – RMSE for Polynomial RBFs with L_1 norm

The reason for integer exponent values β become acceptable is avoiding squaring of the norm used in standard RBF definitions with L_2 norm, directed by Schoenberg-Menger's theorem for conditionally positive semi-definite matrices, as described in [10]. As Figure 3 shows, additional function exponent can be omitted, as described in [6], instead of squaring the norm L_2 in standard RBFs definitions with L_2^2.

The applicability of polynomial RBFs in the description of the lines has been tested in [6], and PRBFs with L_1 norm has proved to have the best properties in their description among several RBF types.

They are very efficient in the 2D global description of the curves also, with whole real number space *IR* acceptable for the choice of the function global shape parameter *c*, as will be shown on Figure 8. Moreover, the accuracy of PRBF 2D description is very high, with RMSE values below required for analytical integration without the error grouping in the point phenomenon. Therefore, they are chosen to be one of the candidates for the description of the curves with discontinuities with standard RBFs with L_2 norm.

2.4 Gibbs and Runge phenomena

There is a problem of the occurrence of oscillations in a global analytic description of objects with discontinuities, known as Gibbs phenomenon, as well as oscillations near boundaries of the description called Runge phenomenon, as described before. The same case is with global descriptions by continuous piecewise functions like radial basis functions.

There are several methods that can be found for the elimination of Gibbs phenomenon; by adding points near discontinuity [11], by post-processing of input data set using spectral filters, [12], and by mappings like conformal mapping, i.e. mapping spectral projection to some other basis, [13].

Regarding Runge's phenomenon of the curve oscillations near boundaries, there are several authors that are proposing methods for its elimination, like spatially variable shape parameters, [14], least squares polynomial approximation on an equidistant grid and Mock-Chebyshev subset interpolation, [15], and varying Gaussian radial basis function exponent with the number of points, extending description range and split range into two boundary layers in [16].

Among above mentioned methods, the procedure of adding points near the point of discontinuity will be observed here with change of Polynomial RBF exponent basis, while other won't be observed. Additionally to added points, the bases of the Polynomial RBFs will be changed near discontinuities in order to describe them without oscillations. In adding the points near the discontinuity there is the limitation in the distance $h_{X,\Omega}$ between points to be added depending on the mapping function chosen, and so is the quality of the description, [6].

Due to the characteristics of global, analytical description defined by points x_j, $j = 1,.., N$, $x \in [a, b]$, the oscillations occur around discontinuities L_l, too, where $l = 1,..., L$, with L equals the number of discontinuities. In order to eliminate those oscillations, it is necessary to include additional information in the interpolation problem about the geometry to be described. In opposite to before mentioned parametric NURB spline methods, analytical solutions of the discontinuities are usually based on the decomposition and Hermite interpolation methods. In this paper, the problem of the discontinuity description will be solved by linearization of the curve near curve breaks bounded by densely added points, with the information about tangents *t*, and normal vectors *n* near discontinuity.

3. Mathematical description of the point discontinuities

The curve discontinuity in some singular point L can be mathematically described as the interruption of all *C* continuities inside the range of the curve definition, along with keeping G^0 continuity. Belonging function $f(x)$, for global description of observed curve discontinuity, needs to have different derivations on the different sides of the discontinuity, as shown below. Figure 4 shows the general case of the curve break with two branches, the left G_L and the right G_D, tangents t_L and t_D, normal vectors n_L and n_D, and curvature radii R_L and R_D, and centres C_L and C_D.

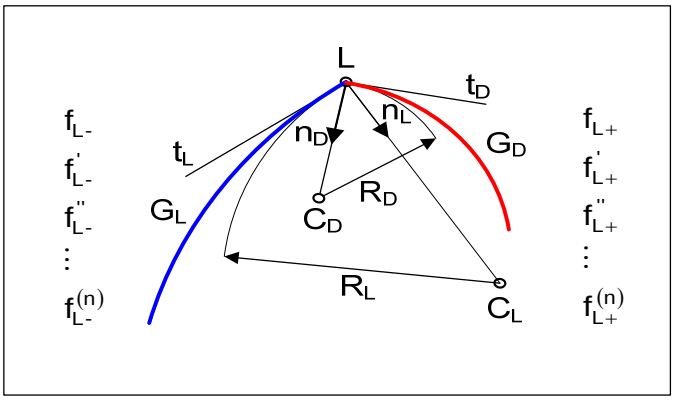

Figure 4 Mathematical description of a curve discontinuity

Analytical function $f(x) \in [a, b]$ with the discontinuity in the point $x = L$ can be written as:

$$f(x) = \begin{cases} f'_{L-}, f''_{L-}, \cdots, f^{(n)}_{L-}, & x \to L- \\ f_{L-} = f_{L+}, & x = L \\ f'_{L+}, f''_{L+}, \cdots, f^{(n)}_{L+}, & x \to L+ \end{cases} \tag{7}$$

Regarding the boundaries of the curve description, their derivations are not defined outside object range. Therefore, the discontinuities are not fully defined on the boundaries, and it is necessary to reduce them by linearization or extension of the description range.

As the measures of the accuracy of the description, global and local errors are defined as RMSE (Root Mean Square Error) and $\mathrm{Err}_{\max}$, for chosen number of input points N:

$$RMSE = \sqrt{\frac{\sum_{j=1}^{N} (f(x_j) - y_j)^2}{N}} \tag{8}$$

where N is the number of input data set, $y_j, j = 1,...,N$ is the output data set of points, and $f(x)$ is radial basis function. And for $\mathrm{Err}_{\max}$ we have:

$$\mathrm{Err}_{\max} = \max(\mathrm{Err}_k), \mathrm{Err}_k = y_k - f(x_k), k = 1, \ldots, N_G \tag{9}$$

where N_G is the number of the points for generalization and evaluation of the description.

The number of points for plotting of the results N_P equals the number of generalization points. Therefore, for some knuckle point L, we have the same function values on the both sides of the discontinuity, but different derivations. That singular point causes oscillations around the discontinuity point L because of the interruption of C continuity, and results in the change of extremes from local minimum to local maximum, with the change of the rhythm of the exchange of the extremes on regular input points, as shown on Figure 1. Besides that, the amplitudes of the oscillations enlarge around the discontinuity point, and it is necessary to reduce them or completely cancel it.

In order to describe the discontinuity with required accuracy it is necessary to add points near it to locally cancel the oscillations or decompose it by translation of the branches of the discontinuity. The required global and local accuracies are set to the values RMSE $\leq 10^{-4}$ and $Err_{max} \leq 10^{-4}$ (m), respectively, to ensure the possibility of RBF integration without occurrence of error grouping in the point, [6].

4. The composition of radial basis functions

The Radial Basis Function networks are enabling piecewise, meshless description of geometry consisting of the composition of the linear sum basis functions as in (2), usually of the same RBF type. Those RBF properties ensure its adjustment to the geometry to be described, with possibility of the change of basis, as will be described in this paper.

The RBF description of the frame with discontinuities using elastic shift method, [6], shows that it is hard to obtain required local description accuracy of $Err_{max} = 10^{-4}$ (m) due to oscillations near the discontinuity point. I.e., it is impossible to control the derivations of the curve near discontinuities when standard RBFs with L_2 norms are used, because of the limitations of a distance between the points h_{min}. Hermite's RBF interpolation, set in the way explained in [10] and [17], does not give acceptable results, too, when applied to curved ship's form, i.e. it is not possible to control the derivations in the discontinuity point. The Gibbs phenomenon is considered in the work [18], too, where adaptive, local approximation is used, and the properties of global RBF description observed near discontinuity depending on shape parameter of RBFs, with the decomposition of the discontinuity in two branches. The composition of Polynomial Radial Basis Functions method with dense description of the discontinuity method will be used in this paper to solve above mentioned description problem, as described in [6].

The validation of the procedure will be performed for the Test Frame No. 1, described on the Table 3 in the Appendix, with discontinuities of the form and flat camber, which description is significant problem for all global computational geometry procedures.

4.1 The Solution of the Description of the Curve with Discontinuities

When the problem of the curve with discontinuities description is observed, there is one method that describes it piecewise continuously, and that is simple, linear interpolation method. Therefore, if we want to describe discontinuities by the composition of the functions, it can be done be linearization of the curve near discontinuity. Corresponding Radial Basis Functions used for discontinuity description need to enable lines description, while another basis function should be used for the description of the rest of the curve, as will be explained further, in the text.

In order to reduce the oscillations and control associate derivations on both discontinuity sides, additional points very near discontinuity need to be added, on small distance $\delta l \to 0$. The curve around discontinuity can then be described by linear and pseudo-linear RB functions, as it is explained in the dissertation [6]. The basic problems with that description, using standard RBFs with L_2 norm, are twofold. The first is connected with worsened convergence when the distance between the input points h_{min} is lowered, and the second is the application of the different basis functions, i.e. the change of basis; linearized RBFs around discontinuity points and smooth RBFs for curved parts. Because of that, the possibility of the global description of discontinuities using the composition of radial basis functions based on L_1 norm is shown in this paper, as in [6], instead of standard RBFs with L_2 norm.

If infinitesimally small parts δl of the curve around discontinuity are observed, it can be seen that curve break represents the discontinuity in the C curvature of the curve, with jump of the values of belonging derivations y', y'', …, and can be approximated by linear function. The discontinuity therefore can be described linearly by straight line, as shown on Figure 5, below, limited by additional points near discontinuity point L, set on some distance δl.

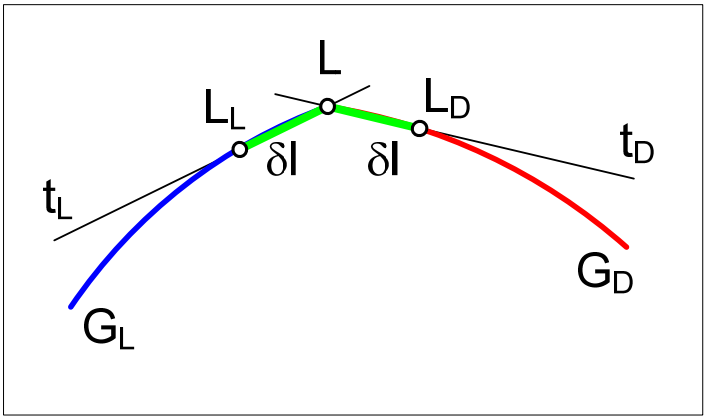

Figure 5 The discontinuity description using lines and dense adding of points

Therefore, it is necessary to include discontinuity points L_l in input data set immediately, where $l \equiv jL = 1,\ldots,L$ is the number of added discontinuity points. When using meshless RBF methods it is possible to do it without limitations, opposite to mesh based methods that require some data organization. The input data set now becomes the set with discontinuities as $X \equiv \{x_1, x_2, \ldots x_{1L}, \ldots, x_j, \ldots, x_{jL}, \ldots, x_{NL}, \ldots, x_{N-1}, x_N\}$.

Beside discontinuity points, it is necessary to add additional points D around discontinuities L_l, too, and enlarge input data set X for the dense points around discontinuities $\{x_{1L}-\delta l, x_{1L}+\delta l, \ldots x_{jL}-\delta l, x_{jL}+\delta l, \ldots x_{NL}-\delta l, x_{NL}+\delta l\}$. Finally, expanded input data set X is obtained, with $N + D + L$ points, that won't be written here, because of its complexity. The position of added points can then be determined by the distance δl from the discontinuity points, on the tangent t_L i t_D lines on the both sides of discontinuity.

Therefore, it is necessary to add points very near to the discontinuity point, as shown on Figure 5, and use linear or pseudo-linear RB function for the description of discontinuity. For the rest of the curve, it is necessary to change the basis and use RBF for smooth description, and use the composition of radial basis functions as:

$$\phi(x) = \phi_s \circ \phi_l \tag{10}$$

where ϕ_s is radial basis function for the description of smooth parts of the curve, and ϕ_l is radial basis function for the description of the flat parts.

The basic condition for the existence of piecewise analytical function, when the curve with discontinuity is described, is the continuity of the range, with C^0 continuity in the vicinity of the discontinuity, and C^n continuity for the smooth parts of the curve. It is also required that the curve description need to have the continuity of the derivations with minimal C^2 continuity. Therefore, the conditions for the choice of RBF functions ϕ_s and ϕ_l are:

$$\phi_s : IR \to IR \in C^n, n \geq 2 \tag{11a}$$

$$\phi_l : IR \to IR \in C^0 \tag{11b}$$

It is shown on Figure 5, that the part of the curve is linearized in the vicinity of the discontinuity, i.e. it is set to C^0, with suitable function ϕ_l used. Curved part of the curve must have minimal C^2 continuity of the description, with the condition of having the second derivation of basis function as:

$$\phi'' \neq 0 \tag{12}$$

For multiple monotonic Polynomial RBFs with L_1 norm, it means that the integer function exponent β values must satisfy condition (13) for required function to produce smooth curve, with limitation in having odd integer values from the definition of PRBFs in (6) as it is shown on the Figure 3:

$$\beta \geq 3 \tag{13}$$

The radial basis functions definition in (4) can now be written for the composition of functions case, defined on the set of points X with N input starting points, L points of discontinuity and D additional points around discontinuity, in the form:

$$\hat{f}(x) = \sum_{i=1}^{N+D} w_i \phi_1\left(\|x, t_i\|; c_1\right) + \sum_{l=1}^{L} w_l \phi_2\left(\|x, t_l\|; c_2\right) \tag{14}$$

where $j = 1, \ldots, N$ are the points of the input data set, with D added points around discontinuity, $l = 1, \ldots, L$ are the discontinuity points, ϕ_1 is the basic RB function for the description of the curved parts of the curve, and ϕ_2 is RB function for the description of the discontinuities.

Additional points have a role of limitation of the influence of the linear Polynomial RBFs to small segments near discontinuity, and the functions ϕ_l for the description of flat parts and discontinuities are set in the discontinuity points L, only. Total number of the points in input data set for the description of the smooth parts of the curve is now $N + D$, and for the simplification their number will be written as N further in the text.

4.2 Additional Points

The additional points D of the description need to be set very near the discontinuity points, on the distances below global description tolerance of 10^{-4} (m), to reduce the error of the description, as described in detail in Chapters from 5 to 8.

This procedure is not always possible for standard RBFs with L_2 norm due to the singularity of interpolating matrix, and the assurance of its good conditioning and inversion, when the distance of input points is very small, [19]. RBFs with L_1 norm are chosen instead, using the composition of radial basis functions with change of basis suitable for the description of the curves with discontinuities.

5. The choice of the functions for the description of discontinuity

When global description of the curves with discontinuities is performed, the need for different basis functions occurs: the smooth RBFs and linear (pseudo-linear) RBFs in the area near discontinuities. But, the usage of the different RBFs creates oscillations also, that can be larger then normal oscillations, and that problem should be solved. In 1991, Sibson and Stone, [20], suggested the procedure based on the search for better bases for conditionally positive definite radial basis functions using reproductive kernels of belonging native spaces, and

Beatson, Light and Billings, [21], performed that procedure for polyharmonic splines, in 2000. The composition of different RBFs should enable simultaneous application of different basis functions, in global description of some geometry without occurrence of oscillations, and that is the main condition for the selection of changeable radial basis functions. The basic function for the description of linear parts of the curve ϕ_l, should be picked first, and than its suitable function ϕ_s for the description of curved parts of the curve.

The properties and the possibility of 2D description of the curves with discontinuities is shown in this chapter for Polynomial RBFs (PRBF), [6], Gaussian RBFs, [10], and Multiquadric RBF (MQ RBF), [22], with L_1 norm, for the description of the Test frame No. 1, as shown in the Table 1, below. These functions have nearly polynomial form, with possibility of linear or pseudo-linear description of flat curve parts, suitable for further computational geometry calculations. The points near discontinuities on the distances 10^{-4} (m) are added to the input point data set in those calculations, on the flat of the side only, as shown in the Table 3, in the Appendix.

Table 1 The results of the description of the Test Frame No. 1, using the composition of RBFs with dense discontinuity description

RBF Type Smooth, ϕ_s	β	c	RBF Type Linear, ϕ_l	β	RMSE	Err_{max}
MQ	1.5	0.01	MQ	0.5	$4.523\cdot10^{-9}$	1.103
	2.5	0.01	MQ	0.5	$3.501\cdot10^{-4}$	1.381
	2.5	0.01	MQ	1	$6.407\cdot10^{-5}$	2.147
Gaussian	3	40	PRBF	1	$1.103\cdot10^{-5}$	$2.692\cdot10^{-2}$
	3	40	Gaussian	1	$5.954\cdot10^{-4}$	$1.301\cdot10^{-2}$
PRBF	1.5	0.01	PRBF	0.5	$6.369\cdot10^{-10}$	$8.898\cdot10^{-1}$
	1.5	0.01	PRBF	1	$1.424\cdot10^{-9}$	1.416
	2.5	0.01	PRBF	0.5	$2.036\cdot10^{-5}$	1.164
	2.5	0.01	PRBF	1	$9.251\cdot10^{-5}$	$8.338\cdot10^{-1}$
	3	0.01	PRBF	1	$5.251\cdot10^{-3}$	$1.196\cdot10^{-2}$
	3	3.08	PRBF	1	$1.424\cdot10^{-4}$	$2.388\cdot10^{-4}$

It can be concluded from the results in the Table 1 that PRBFs and Gaussian RBFs, with function exponents $\beta = 3$, are suitable for the description of discontinuities. It can be noticed in it, that PRBF with $\beta = 3$ have compatible function PRBF with $\beta = 1$ and that is computationally the most suitable combination of functions that will be further investigated.

In order to obtain better shape parameter c value of the smoothing function ϕ_s, the belonging sensitivity diagram c – RMSE is done, while c for linear function ϕ_l is fixed to 0.01 in this case. The value $c = 3.08$ is determined, what gives the accuracy values RMSE = $1.424\cdot10^{-4}$ and $Err_{max} = 2.388\cdot10^{-4}$ (m), with the values very near required global and local accuracy values.

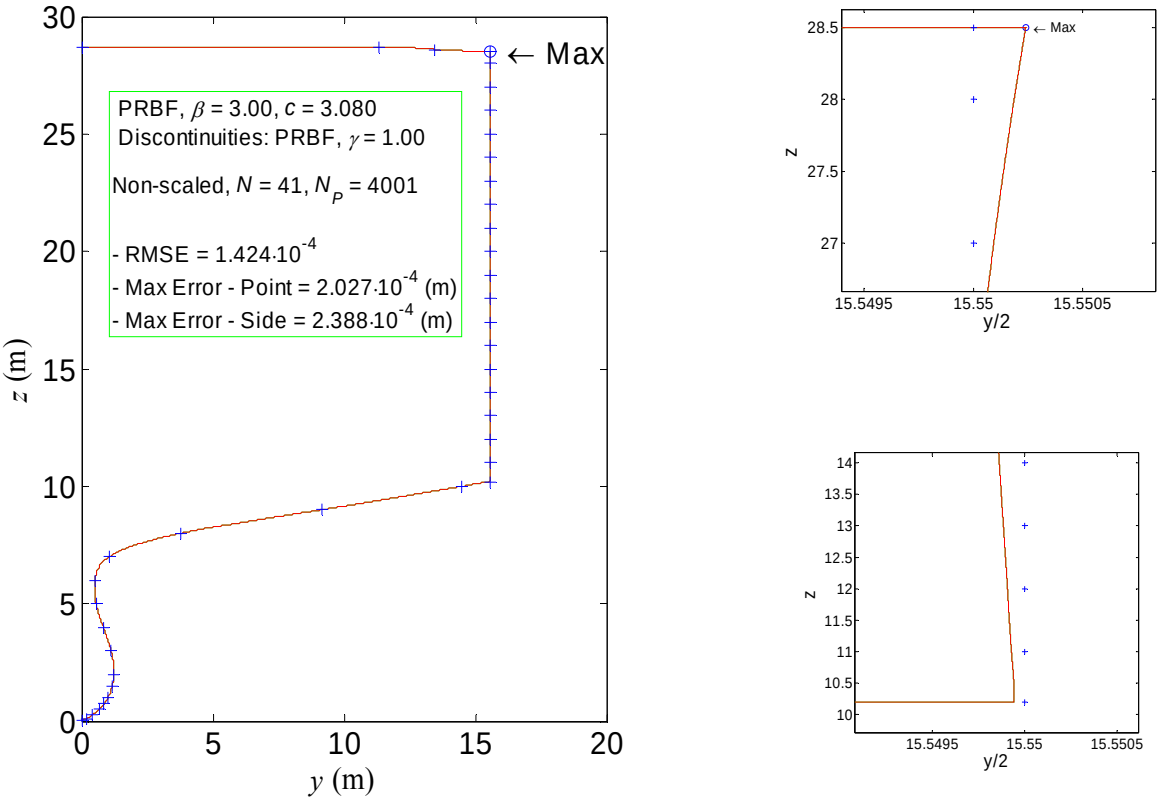

Figure 6 The description of Test Frame No. 1 with camber and knuckles, using PRBF composition with $\beta = 3$ for curved frame parts and $\beta = 1$ for discontinuities description

Figure 6, above, shows the description of the Test Frame No. 1, with knuckles and camber, using PRBF composition, with exponent $\beta = 3$ for the description of smooth parts of the curve and $\beta = 1$ for the description of the discontinuities. It is shown that PRBF with $\beta = 3$ is suitable function for the smooth description of the frame with discontinuities, compatible with the function PRBF with $\beta = 1$ for the description of flat parts of the frame and discontinuities.

Nevertheless, the choice of polynomial RBFs limits the applicability of this procedure to 2D problems, concerning the limitations of polynomial descriptions from Mairhuber-Curtis theorem, [10], and the corresponding solution for 3D geometries with discontinuities is still to be found.

6. Natural description of the flat parts of the curve

As the side of the Test Frame No. 1 is flat, only two points are needed for side description in the case of linear description, as shown in the Table 4, in the Appendix. This description represents natural description of the straight line with minimal number of points. Therefore, all other points in the starting input data set, but two points, are left out from it for flat side description, with dense points for the description of frame brakes. After that, the description of the test frame with knuckles and camber is tested for RBF description by the composition of PRBF functions for new input data set. Belonging statement for PRBFs with the composition of basis functions is then:

$$\hat{f}(x) = \sum_{i=1}^{N} w_i \phi_1 \left(\left| x, t_i \right|^3 ; c_1 \right) + \sum_{l=1}^{L} w_l \phi_2 \left(\left| x, t_l \right| ; c_2 \right) \tag{15}$$

It can be seen that the function used for the description of smooth curve parts is cubic spline, [19], and the function for the description of flat parts of the frame is linear function. Those functions have L_1 norm as the argument, i.e. absolute value of the difference between x and x_i, $\left| x - x_i \right|$.

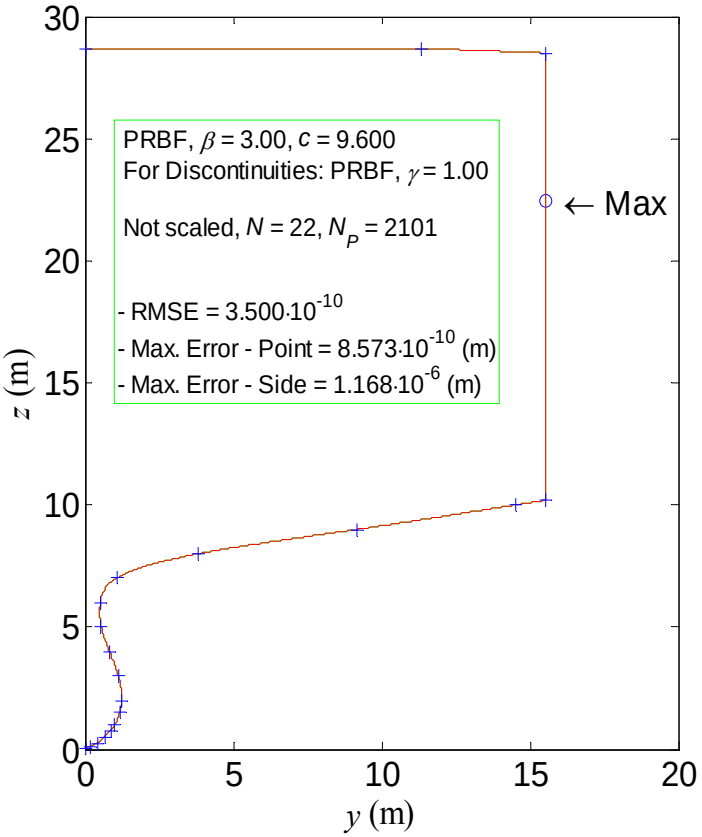

Figure 7 The description of the Test Frame No. 1 with camber and knuckles, by composition of PRBF functions with $\beta = \{3, 1\}$

After calculation by PRBF composition, with $\beta = 3$ and $c = 9.6$ for smooth parts, and $\beta = 1$ and $c = 0$ for the description of flat parts and discontinuities, following values of errors are obtained for the Test Frame No. 1: RMSE = $3.5 \cdot 10^{-10}$ and $\mathrm{Err}_{\max} = 1.168 \cdot 10^{-6}$ (m). It can be seen that local description error $\mathrm{Err}_{\max}$ is significantly below required 10^{-4} (m), and therefore the condition of local precision of the description is fulfilled.

Figure 7, above, shows natural ship description of the ship frame with discontinuities using the composition of PRBFs, with 1 point added near each frame knuckle, with left out points for the side description.

Besides that, the composition of basis functions PRBFs with $\beta = \{3, 1\}$ and adjusted input data set, removes the region of global accuracy of the description from the range of 10^{-3} to 10^{0}, to the accuracy range from 10^{-9} to 10^{-6}. I.e., whole region of the shape parameter c for composition of polynomial radial basis functions is acceptable as can be seen on Figure 8, below.

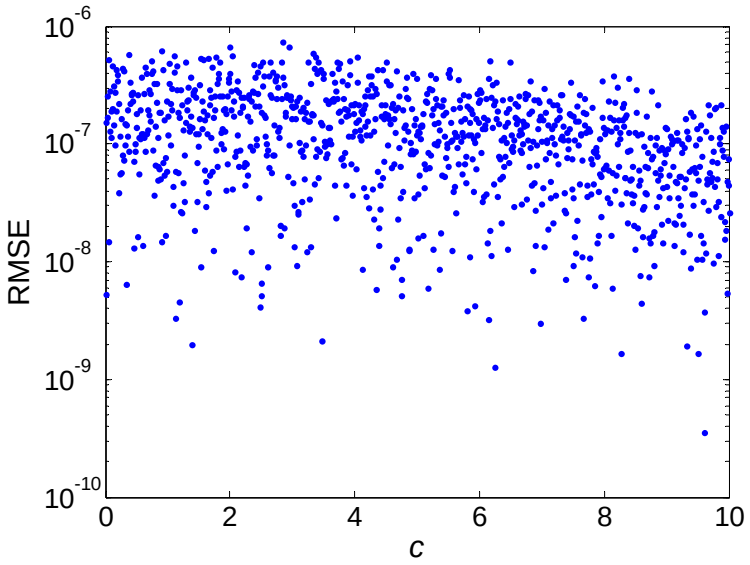

Figure 8 The sensitivity diagram of global shape parametar c for the test frame description by composition of PRBFs with $\beta = \{3, 1\}$

Additionally, it can be concluded that it is possible to omit shape parameter c in a natural description by PRBFs function composition with $\beta = \{3, 1\}$, in some cases. Pure polynomial description can be obtained in this way, without additive constant in the function definition, thus eliminating the search for optimal shape parameter c. Besides that, the number of input data set points is reduced when flat parts exist in the frame curve description. Moreover, the composition of PRBFs gives robust description with very high accuracy, which is required for the direct analytical integration calculations where grouping of error in a point has to be avoided, [6]. Therefore, the statement (15) can be written as:

$$\hat{f}(x) = \sum_{i=1}^{N} w_i \phi_1\left(\left|x, t_i\right|^3\right) + \sum_{l=1}^{L} w_l \phi_2\left(\left|x, t_l\right|\right), \quad x \in IR^s \tag{16}$$

Therefore, it is not necessary to introduce function shape parameter c, i.e. the description accuracy does not significantly change by c, as shown on Figure 8, above.

Additionally, for PRBFs there holds:

$$\hat{f}(x) = \sum_{i=1}^{N} w_i \left|x - t_i\right|^3 + \sum_{l=1}^{L} w_l \left|x - t_l\right|, \quad x \in IR^s \tag{17}$$

This conclusion connects Polynomial RBFs with Radial Power Functions which are classified as polyharmonic splines, [19], in theory, i.e. they also do not depend on shape parameter c. The statement (17) explains and confirms the name Polynomial RBFs, because cubic spline is obtained as the result, with the argument consisting of the absolute value of the difference between input data set points and the points of centres for the development of RBF description.

The summation of the terms for each polynomial exponent finally gives cubic polynomial written by coefficients as:

$$f(x) = C_{j3}x^3 + C_{j2}x^2 + C_{j1}x + C_{j0}, \; j = 1,\ldots,N \tag{18}$$

where C_{j3}, C_{j2}, C_{j1} and C_{j0} are the polynomial coefficients of the cubic for j–th segment of the description, i.e. for $x \in [t_j, t_{j+1}]$ or $x \in [x_j, x_{j+1}]$ when centers vector t coincide with vector x.

Analytical description by cubic polynomials, (18), is very simple and robust, and beside the solution of the oscillations of global interpolation description, enables further analytical calculations of ship's hydrostatic properties, instead of numeric integration methods used for their calculations, together with the solution of the intersection of the ship's geometry with waterlines.

7. The accuracy of the description near added points

In order to achieve the linearization of the description near discontinuities, it is necessary to add points densely around them. The positions of those points have not been observed yet, and that will be done in this chapter. Consequently, the sensitivity of the description by the composition of PRBFs with $\beta = \{3, 1\}$ and $c = 9.6$ on the position of added points near discontinuities is investigated, i.e. their direction and the distance from the discontinuity points for Test Frame No. 1, from Figure 7. The sensitivity is tested for vertical Δz and horizontal distances Δy from discontinuity points, as shown in the Table 2 and Figure 9, below.

Table 2 The influence of the position of additional points near discontinuity on the results of the description of the Test Frame No. 1

Added Points, Vertical Translation Δz			Added Points, Horizontal Transl. Δy, $\Delta z = 10^{-4}$		
Transl.	RMSE	Err_{max}	Transl.	RMSE	Err_{max}
10^{-1}	$5.928 \cdot 10^{-8}$	$5.091 \cdot 10^{-3}$			
10^{-2}	$6.465 \cdot 10^{-8}$	$8.140 \cdot 10^{-5}$			
10^{-3}	$1.920 \cdot 10^{-8}$	$9.030 \cdot 10^{-7}$	10^{-4}	$2.110 \cdot 10^{-9}$	$4.576 \cdot 10^{0}$
10^{-4}	$3.500 \cdot 10^{-10}$	$1.168 \cdot 10^{-6}$	10^{-5}	$7.773 \cdot 10^{-9}$	$4.576 \cdot 10^{-1}$
10^{-5}	$2.969 \cdot 10^{-8}$	$8.495 \cdot 10^{-6}$	10^{-6}	$3.141 \cdot 10^{-9}$	$4.576 \cdot 10^{-2}$
10^{-6}	$5.630 \cdot 10^{-7}$	$5.662 \cdot 10^{-5}$	10^{-9}	$3.795 \cdot 10^{-9}$	$4.673 \cdot 10^{-5}$
10^{-7}	$1.371 \cdot 10^{-5}$	$4.046 \cdot 10^{-4}$			
10^{-8}	$8.849 \cdot 10^{-5}$	$4.077 \cdot 10^{-3}$			
10^{-9}	$1.129 \cdot 10^{-4}$	$2.467 \cdot 10^{-2}$			

From the results in Table 2, it can be seen that the accuracy of the description depends on the coincidence of added points with the tangents around the discontinuity points.

The results for different positions of the added points for Test Frame No. 1, from Table 3 in the Appendix, show that the horizontal translation of added points Δy is more significant, because it shows the difference from the tangent slopes in the points of discontinuities. Therefore, the local description error Err_{max} grows linearly with Δy, while RMSE does not depend significantly on Δy.

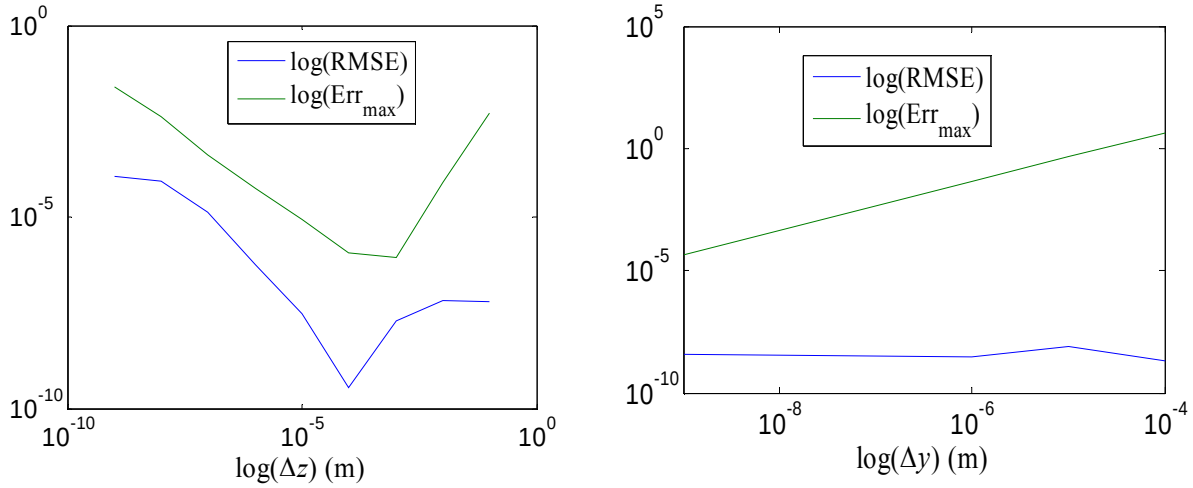

Figure 9 The influence of the position of additional points near discontinuity on the results of the Test Frame No. 1 description

It can be concluded that additional points need to be set on the tangent lines near discontinuities, with the distance from the discontinuity points around required accuracy tolerance of 10^{-4} (m).

Therefore, for the 2D ship geometry description by the composition of PRBFs with dense point description of discontinuities, it is necessary to have additional information about the tangents on the both sides of discontinuity. Anyway, this method requires less amount of information compared to usual RBF description or Hermite RBF method, due to reduction of the number of points for flat parts description.

The necessary number of points required for the description by the composition of Polynomial Radial Basis Functions with dense point discontinuity description is therefore $N + L + D$, where N is the number of the points at the beginning, L is the number of discontinuity points, and D is the number of added points near discontinuities with the slope of the tangents near discontinuity points. The number of densely added points D can vary depending on the case, as will be shown in the description of Test Frame No. 2, in the next chapter.

8. The example of the description of a test frame from a planning boat

Additional example for showing the applicability of the global 2D description of ship's geometry by composition of Polynomial RBFs with $\beta = \{3, 1\}$ and the dense points near discontinuity, the description of the frame of the planning boat will be shown in this chapter, defined as Test Frame No. 2, described in the Table 5, in the Appendix. It represents the frame of a planning boat with several knuckles and curved camber, as shown on Figure 10, with the interchange of curved and flat parts of the frame curve.

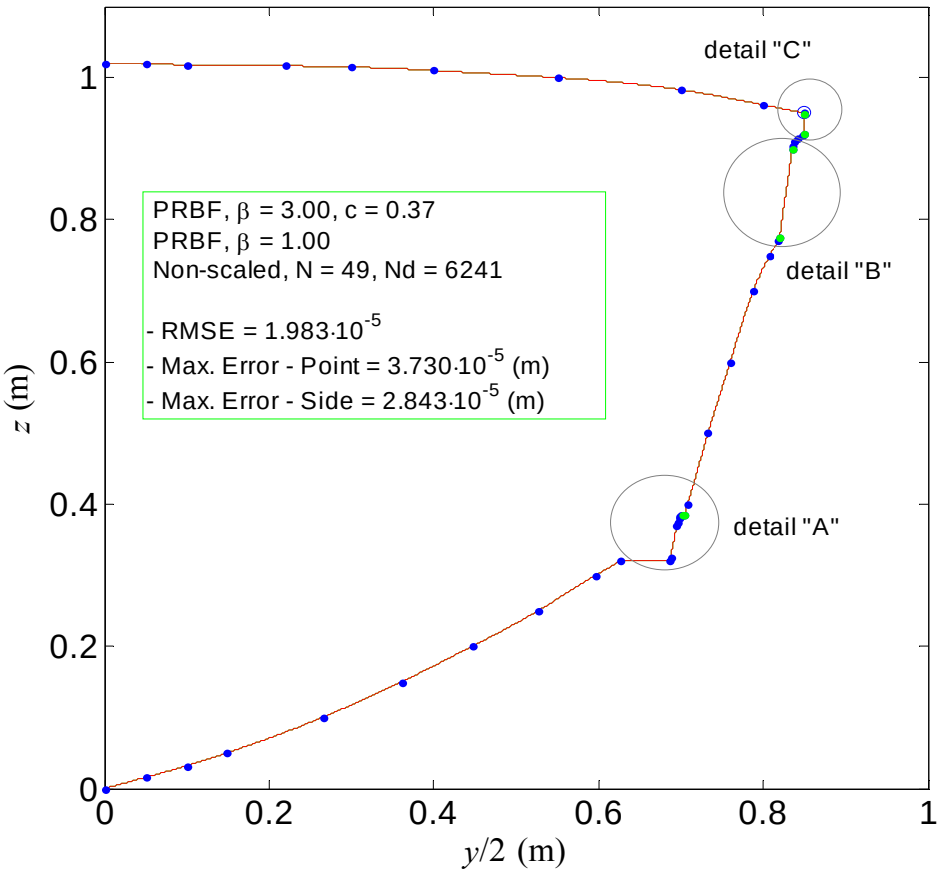

Figure 10 The description of the Test Frame No. 2, using the composition of Polynomial RBFs with $\beta = \{3, 1\}$ and dense knuckles description (green)

At the beginning Test Frame No. 2 is defined with the input set of $N = 37$ points. After that it is expanded for the additional $L = 6$ points for discontinuities description and $D = 6$ additional points near discontinuities for their dense description, in order to enable the application of the composition of PRBFs method with $\beta = \{3, 1\}$. One, two or none additional points, including discontinuity points have to be added to the input data set on the distance of $1 \cdot 10^{-4}$ (m) and $2 \cdot 10^{-4}$ (m), thus forming input data set of $N = 49$ in total, as shown in the Table 5 in the Appendix.

It can be seen that very good global accuracy of RMSE = $1.983 \cdot 10^{-5}$ and local accuracy of $Err_{max} = 3.73 \cdot 10^{-5}$ (m) is obtained by using PRBF composition with $\beta = \{3, 1\}$ and dense discontinuity description, thus fulfilling required accuracy criterion of 10^{-4}.

Regarding the fact that Test Frame No. 2 has very complex geometry with 6 knuckles, several curvature and flatness changes, it can be concluded that new analytical 2D ship's geometry description method using PRBFs has excellent efficiency of the description for curves with discontinuities. Moreover, there is no need for any additional point near discontinuities in some cases with the tangent near 90°.

Considering the complexity of the problem, it was necessary to include shape parameter c of radial basis function ϕ_s for smooth parts description in this case, with $c = 0.37$, while for radial basis function ϕ_l for flat parts description c can be omitted.

Added points near discontinuities for the Test Frame No. 2 are shown in Figure 10, with the details „A“, „B“ and „C“, depending on the case as shown on Figures 11 and 12.

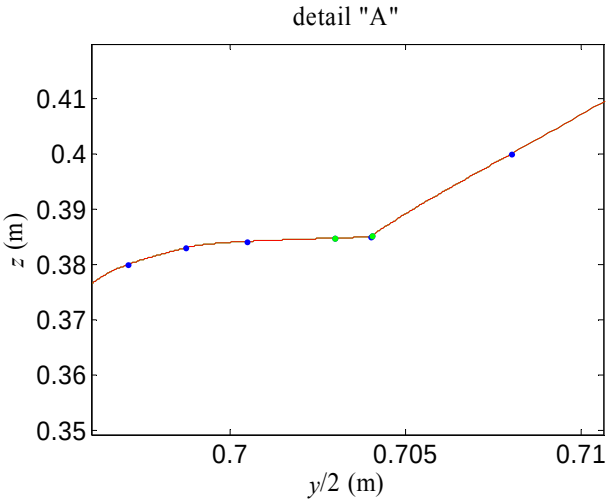

Figure 11 The detail of the description of the Test Frame No. 2, with two points around the knuckle, one from each side of the knuckle

In the case of large differences in the slopes of the tangents of the discontinuity branches t_L and t_D it is necessary to add two points, one on the each side of the discontinuity, as shown by magnification „A“, on Figure 11.

Further, in the case of flat frame parts description it is necessary to add one point on the each knuckle of the straight line on the frame side, as shown on the magnifications „B“ and „C“, on Figure 12.

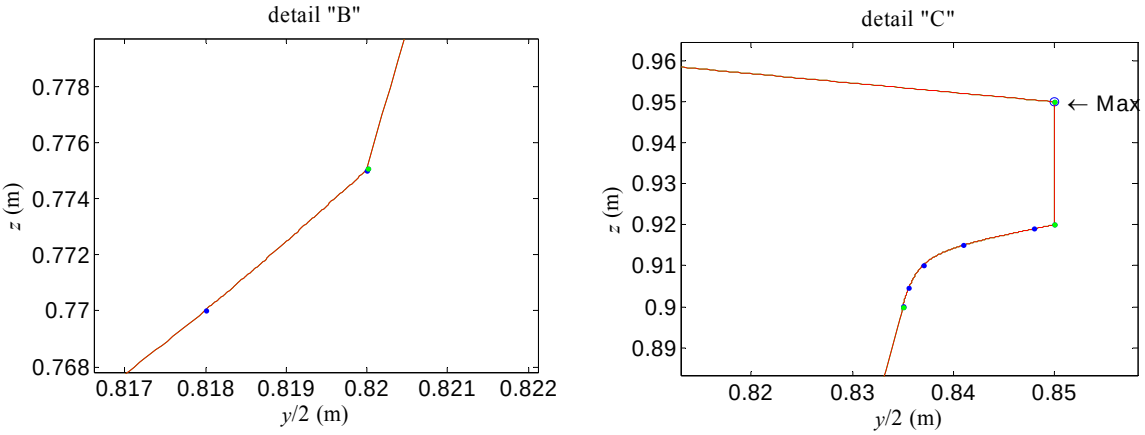

Figure 12 The details “B” and “C” of the description of the Test Frame No. 2, with one point around the knuckle in order to describe flat part of the frame

In all cases, the points are set on the distance 10^{-4} (m) from the discontinuity point, along the z axis. Finally, in the case of the flat part of the frame near or on the 90° slope it is not necessary to add any point to achieve flat description, as shown on Figure 10.

Additionally, in order to describe boundaries of the frame with required accuracy and without oscillations, the first point of the frame at the bottom is set as discontinuity too, thus solving Runge phenomenon, also, as it can be seen on Figures 6, 7 and 10, where Test Frames No. 1 and 2 are described.

It can be concluded that it is possible to use the Composition of compatible Polynomial RBFs with dense points method for global description of the curves with discontinuities and multiple changes of smooth and flat parts, with very high accuracy.

9. Conclusion

The composition of compatible cubic-linear polynomial radial basis functions with dense description of curve knuckles is the solution of the problem of global 2D ship's geometry description for frames with discontinuities. The linearization of the curve near discontinuities, and usage of L_1 norm instead of L_2, enables the description of discontinuities by linear Polynomial RBFs, very near to discontinuity points.

Furthermore, smooth parts of the curve can be described by cubic Polynomial RBFs, without occurrence of additional oscillations, known as Gibbs and Runge phenomena. As the final result of that description, cubic piecewise polynomials are obtained, giving direct, explicit and very accurate description of the curve with discontinuities, representing complete solution of 2D ship's computational geometry problems.

This solution of the analytical description of the curve with discontinuities is the simplest possible and represents yet another example of Occam's razor applied, consisting of the composition of linear and cubic polynomial RBFs.

It can be concluded comprehensively that this solution represents complete analytical solution of global 2D geometry reconstruction problem for curves with discontinuities. Being essentially analytical, the composition of cubic-linear polynomial radial basis functions enables direct, analytical procedure of integration under the curve thus solving all 2D ship's computational geometry problems, as will be described in detail in future paper.

In order to solve ship's geometry problems completely, it is necessary to solve the problem of the reconstruction of 3D ship geometry with discontinuities, too, and that will be the subject of the future research of this authors in the field of ship's computational geometry.

REFERENCES

[1] CHAPMAN, F. H.: Architectura Navalis Mercatoria, Första sidan till „Tractat om Shepps-Byggeriet“, 1775.

[2] EULER, L.: Scientia Navalis, 1749.

[3] TAYLOR, D. W.: Calculations of Ships' Forms and Light Thrown by Model Experiments upon Resistance, Propulsion and Rolling of Ships, Intl Congress of Engineering, San Francisco, 1915..

[4] PIEGL, L., TILLER, W.: The NURBS Book, Springer-Verlag, 1997.

[5] BAN, D., BLAGOJEVIĆ, B., BARLE, J.: Ship geometry description using global 2D RBF interpolation, Shipbuilding, Zagreb, 233-242, 2010.

[6] BAN, D.: Analytical Ship Geometry Description using Global RBF Interpolation, PhD disertation, Rijeka, 2012.

[7] LIPSCHUTZ, M.: Theory and Problems of Differential Geometry, Schaum's Outline Series, McGraw-Hill, Inc., 1969.

[8] ARONSZAJN, N.: "Theory of reproducing kernels", Trans. Amer. Math. Soc. 68, p. 337-404, 1950.

[9] POGGIO, T., GIROSI, F.: Networks and the best approximation property, MIT, AI Laboratory, MIT, Cambridge, MA, A. I. Memo No. 1164, C.B.I.P. Paper No. 45, 1989.

[10] FASSHAUER, G. E.: Meshfree Approximation Methods with MATLAB, Interdisciplinary Mathematical Sciences – Vol. 6, World Scientific, 2007.

[11] SARRA, S. A.: The MATLAB Postprocessing Toolkit, 2008.

[12] TREFETHEN, L. N.: Spectral methods in MATLAB, SAIM, Philadelphia, 2000.

[13] VANDEVEN, H.: Family of spectral filters for discontinuous problems, SIAM Journal of Scientific Computing, 6:159-192, 1991.

[14] FORNBERG B., ZUEV J.: The Runge phenomenon and spatially variable shape parameters in RBF interpolation, Computers and Mathematics with Applications, pp. 379-398, 2007.

[15] BOYD J. P., XU F.: Divergence (Runge Phenomenon) for least-square polynomial approximation on an equispaced grid and Mock-Chebyshev subset interpolation, Applied Mathematics and Computation, pp. 158-168, 2009.

[16] BOYD J. P.: Six strategies for defeating Runge Phenomenon in Gaussian radial basis functions on finite interval, Computers and Mathematics with Applications, pp. 3108-3122, 2010.

[17] WU, Z.; Hermite-Birkhoff interpolation of scattered data by RBFs, 1992.

[18] JUNG, J. H.: A note on Gibbs phenomenon with multiquadric radial basis functions, Applied numerical mathematics 57, pp. 213-229, 2007.

[19] WENDLAND, H.: "Scattered Data Approximation", Cambridge University Press (Cambridge), 2005.

[20] SIBSON R., STONE, G.: Computation of thin-plate splines, SIAM J. Sci. Statist. Comput. 12, pp. 1304-1313, 1991.

[21] BEATSON, R. K., LIGHT, W. A., BILLINGS, S.: Fast evaluation of radial basis functions: methods for two-dimensional polyharmonic splines, SIAM J. Sci. Comput. 22, pp. 1717-1740, 2000.

[22] HARDY, R. L.: "Multiquadric equations to topography and other irregular surfaces", J. Geophys. Res. 76, p. 1905-1915, 1971.

APPENDIX

The points coloured red in the tables below are designating added points near discontinuities, while blue marking designates discontinuity points.

Table 3 Offset table of Test Frame No. 1 with knuckles and flat camber

	z	y/2
1	0.0408	0
2	0.1	0.1758
3	0.25	0.4228
4	0.5	0.6857
5	0.75	0.8688
6	1	1.005
7	1.5	1.173
8	2	1.2329
9	3	1.1198
10	4	0.8255
11	5	0.5456
12	6	0.5218
13	7	1.0714
14	8	3.7948
15	9	9.1507
16	10	14.5066
17	10.1948	15.55
18	10.1949	15.55
19	11	15.55
20	12	15.55
21	13	15.55

	z	y/2
22	14	15.55
23	15	15.55
24	16	15.55
25	17	15.55
26	18	15.55
27	19	15.55
28	20	15.55
29	21	15.55
30	22	15.55
31	23	15.55
32	24	15.55
33	25	15.55
34	26	15.55
35	27	15.55
36	28	15.55
37	28.4999	15.55
38	28.5	15.55
39	28.6	13.445
40	28.7	11.34
41	28.7	0

Table 4 Test Frame No. 1 with knuckles and flat camber, without side points

	z	y/2
1	0.0408	0
2	0.1	0.1758
3	0.25	0.4228
4	0.5	0.6857
5	0.75	0.8688
6	1	1.005
7	1.5	1.173
8	2	1.2329
9	3	1.1198
10	4	0.8255
11	5	0.5456

	z	y/2
12	6	0.5218
13	7	1.0714
14	8	3.7948
15	9	9.1507
16	10	14.5066
17	10.1948	15.55
18	10.1949	15.55
19	28.4999	15.55
20	28.5	15.55
21	28.7	11.34
22	28.7	0

Table 5 Offset table of Test Frame No. 2 of planning boat with discontinuities and curved camber

	z	y/2
1	0	0
2	0.0155	0.05
3	0.032	0.1
4	0.05	0.1487
5	0.1	0.265
6	0.15	0.361
7	0.2	0.447
8	0.25	0.527
9	0.3	0.597
10	0.32	0.627
11	0.3201	0.687
12	0.3202	0.687018
13	0.324	0.6876
14	0.37	0.6948
15	0.375	0.6958
16	0.38	0.6971
17	0.383	0.69873
18	0.3842	0.7005
19	0.3848	0.703
20	0.385	0.704
21	0.3852	0.70404
22	0.4	0.708
23	0.5	0.733
24	0.6	0.76
25	0.7	0.788

	z	y/2
26	0.75	0.808
27	0.77	0.818
28	0.775	0.82
29	0.7751	0.82001
30	0.8999	0.83499
31	0.9	0.835
32	0.9001	0.83501
33	0.9045	0.8356
34	0.91	0.837
35	0.915	0.841
36	0.919	0.848
37	0.92	0.85
38	0.9201	0.85
39	0.9499	0.85
40	0.95	0.85
41	0.9615	0.8
42	0.9828	0.70
43	1.00	0.55
44	1.01	0.4
45	1.015	0.3
46	10.167	0.22
47	10.182	0.1
48	10.192	0.05
49	1.02	0

Submitted: 07.09.2013.

Accepted: 07.04.2014.

Dario Ban, Branko Blagojević
University of Split, Faculty of Electrical Engineering, Mechanical Engineering and Naval Architecture (FESB), R. Boskovica 32, 21000 Split, Croatia
e-mail: dario.ban@fesb.hr; bblag@fesb.hr
Bruno Čalić,
University of Rijeka, Faculty of Engineering, Vukovarska 58, 51000 Rijeka, Croatia
e-mail: bruno.calic@riteh.hr